

# Electrogenicity of the Sodium Transport Pathway in the Na,K-ATPase Probed by Charge-Pulse Experiments

Ingo Wuddel and Hans-Jürgen Apell

Department of Biology, University of Konstanz, Konstanz, Germany

**ABSTRACT** A charge-pulse technique was designed to measure charge movements in the Na-transport mode of the Na,K-ATPase in membrane fragments adsorbed to a planar lipid bilayer with high time resolution. 1)  $\text{Na}^+$  transport was measured as a function of membrane potential, and 2) voltage-dependent extracellular ion binding and release were analyzed as a function of  $\text{Na}^+$  concentration and membrane potential. The results could be fitted and explained on the basis of a Post-Albers cycle by simulations with a mathematical model. The minimal reaction sequence explaining the electrogenicity of the pump consists of the following steps:  $(\text{Na}_3)\text{E}_1\text{-P} \leftrightarrow \text{P-E}_2(\text{Na}_3) \leftrightarrow \text{P-E}_2(\text{Na}_2) \leftrightarrow \text{P-E}_2(\text{Na}) \leftrightarrow \text{P-E}_2$ . The conformational change,  $\text{E}_1$  to  $\text{E}_2$ , is electrogenic ( $\beta_0 \leq 0.1$ ) and the rate-limiting step of forward  $\text{Na}^+$  transport with a rate constant of  $25 \text{ s}^{-1}$  ( $T = 20^\circ\text{C}$ ). The first ion release step,  $\text{P-E}_2(\text{Na}_3) \leftrightarrow \text{P-E}_2(\text{Na}_2)$ , is the major charge translocating process ( $\delta_0 = 0.65$ ). It is probably accompanied by a protein relaxation in which the access structure between aqueous phase and binding site reduces the dielectric distance. The release of the subsequent  $\text{Na}^+$  ions has a significantly lower dielectric coefficient ( $\delta_1 = \delta_2 = 0.2$ ). Compared with other partial reactions, the ion release rates are fast ( $1400 \text{ s}^{-1}$ ,  $700 \text{ s}^{-1}$ , and  $4000 \text{ s}^{-1}$ ). On the basis of these findings, a refined electrostatic model of the transport cycle is proposed.

## INTRODUCTION

The Na,K-pump is an essential protein in all animal cells where it maintains concentration gradients across the cytoplasmic membrane for potassium, which mainly controls the membrane potential, and for sodium, which generates the driving force for many secondary active transport systems. The pumping process involves a sequence of conformational transitions and ion binding and release reactions (Glynn, 1985; Jørgensen and Andersen, 1988; Läuger, 1991). The free energy of hydrolysis of one ATP molecule is used to extrude three  $\text{Na}^+$  ions from the cytoplasm in exchange for two  $\text{K}^+$  ions from the extracellular aqueous phase. The transport of one net charge per cycle across the membrane drives an electric current and thus indicates the existence of one or more electrogenic reaction steps. In contrast to other reaction steps, electrogenic steps are controlled not only by ion and substrate concentrations but also by the transmembrane electric field (Läuger and Apell, 1988; Apell, 1989).

The pump cycle of the Na,K-ATPase can be described by the generally accepted Post-Albers cycle (Fig. 1), in which four partial reactions are electrogenic: the cytoplasmic  $\text{Na}^+$  binding,  $\text{E}_1 + 3 \text{Na}_{\text{cyt}} \rightarrow \text{Na}_3\text{E}_1$ , (Goldshleger et al., 1987; Stürmer et al., 1991; Heyse et al., 1994); the conformational transition,  $(\text{Na}_3)\text{E}_1\text{-P} \rightarrow \text{P-E}_2(\text{Na}_3)$  as well as the subsequent release of  $\text{Na}^+$  ions,  $\text{P-E}_2(\text{Na}_3) \rightarrow \text{P-E}_2 + 3 \text{Na}_{\text{ext}}$  (Nakao and Gadsby, 1986, 1989; Läuger and Apell, 1988; Borlinghaus et al., 1987; Stürmer et al., 1991; Stürmer and Apell,

1992; Gadsby et al., 1993; Sagar and Rakowski, 1994; Heyse et al., 1994); and finally the extracellular binding of  $\text{K}^+$  ions,  $\text{P-E}_2 + 2 \text{K}_{\text{ext}} \rightarrow \text{P-E}_2(\text{K}_2)$ , (Rakowski et al., 1991; Stürmer et al., 1991; Vasilets et al., 1991; Sagar and Rakowski, 1994).

Different preparations and techniques have been used to analyze the electrogenicity of the major electrogenic reaction sequence  $(\text{Na}_3)\text{E}_1\text{-P} \rightarrow \dots \rightarrow \text{P-E}_2$ . Nakao and Gadsby (1986) investigated time-dependent pump currents in isolated heart cells using the whole-cell recording. They could interpret their data with a model in which the (single) electrogenic step was the conformational transition of the phosphoenzyme  $(\text{Na}_3)\text{E}_1\text{-P} \rightarrow \text{P-E}_2(\text{Na}_3)$ . In 1989 the same authors demonstrated an interaction between extracellular  $\text{Na}^+$  concentration and membrane voltage, which was compatible with a model in which the occupation of the extracellular  $\text{Na}^+$  binding sites is modulated by membrane voltage (Nakao and Gadsby, 1989). The fluorescence dye RH 421, which detects changes in the local electric field produced by electrogenic charge movements within the Na,K-ATPase, was used to show that extracellular  $\text{Na}^+$  binding is an electrogenic event (Stürmer et al., 1991) and that it occurs in at least two charge-moving steps,  $(\text{Na}_3)\text{E}_1\text{-P} \rightarrow \text{P-E}_2(\text{Na}_2)$  and  $\text{P-E}_2(\text{Na}_2) \rightarrow \text{P-E}_2$  (Stürmer and Apell, 1992). Direct electrical measurements with membrane fragments coupled to planar lipid bilayers allowed the determination of dielectric coefficients of two partial reactions,  $(\text{Na}_3)\text{E}_1\text{-P} \rightarrow \text{P-E}_2(\text{Na}_2)$  and  $\text{P-E}_2(\text{Na}_2) \rightarrow \text{P-E}_2$ , to be 0.75 and 0.2, respectively, in renal Na,K-ATPase (Heyse et al., 1994). Recently the charge movements of  $\text{Na}^+$  translocation in a giant cardiac-membrane patch were analyzed (Hilgemann, 1994). The author presented findings compatible with a model in which the major electrogenic event is the release of the first ion from state  $\text{P-E}_2(\text{Na}_3)$ , whereas the successive reaction,  $\text{P-E}_2(\text{Na}_2) \rightarrow \text{P-E}_2 + 2 \text{Na}_{\text{ext}}$ , is only

Received for publication 19 April 1995 and in final form 14 June 1995.

Address reprint requests to Hans-Jürgen Apell, University of Konstanz, Postfach 5560 M635, D-78434 Konstanz, Germany. Tel.: 011-49-7531-88-2253; Fax: 011-49-7531-88-3183; E-mail: hjapell@dg1.chemie.uni-konstanz.de.

© 1995 by the Biophysical Society

0006-3495/95/09/909/13 \$2.00

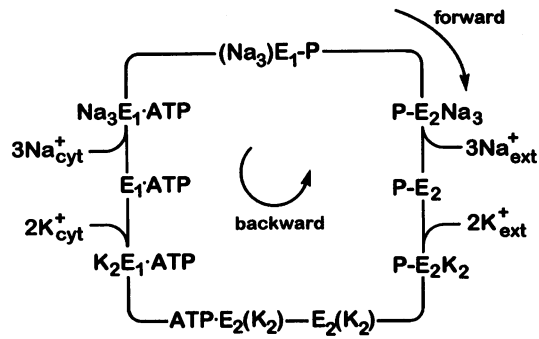


FIGURE 1 Post-Albers cycle of the physiological pump mechanism of the Na,K-ATPase.  $E_1$  and  $E_2$  are the two principal conformations of the enzyme in which the ion-binding sites are presented to the cytoplasm and extracellular medium, respectively. In the occluded states,  $(Na_3)E_1-P$ ,  $E_2(K_2)$  and ATP  $E_2(K_2)$ , the ions are unable to exchange with either aqueous phases.

weakly voltage-dependent. The corresponding dielectric coefficients were determined to be 0.67 and 0.26.

The fact that the transport properties depend on the transmembrane electric field was used in this work to modulate the activity of the pump in addition to ion and substrate concentrations. To change the membrane voltage in a time scale, which is fast compared to typical time constants of the transport processes in the protein, we applied a charge-pulse method to a compound membrane system that consisted of a planar lipid bilayer and adsorbed flat membrane fragments with a high concentration of Na,K-ATPase molecules purified from rabbit kidney (Borlinghaus et al., 1987). The charge-pulse technique was introduced originally to study current relaxations in membranes containing hydrophobic ions and carriers (Benz and Läuger, 1976; Barth et al., 1994). By this method it was possible to perform voltage-jump experiments with isolated Na,K-ATPase, which previously had been possible only in whole-cell and giant-patch studies. Analysis of electric currents induced by ATP-concentration and voltage-jump experiments allowed an accurate determination of the dielectric coefficients of the reaction sequence  $(Na_3)E_1-P_1 \rightarrow P-E_2(Na_3) \rightarrow P-E_2(Na_2) \rightarrow P-E_2(Na) \rightarrow P-E_2$ .

## MATERIALS AND METHODS

### Materials

L-1,2-diphytanoyl-3-phosphatidylcholine was obtained from Avanti Polar Lipids (Birmingham, AL), and sodium dodecyl sulfate was obtained from Pierce Chemical (Rockford, IL). Phosphoenolpyruvate, pyruvate kinase, lactate dehydrogenase, reduced nicotinamide adenine dinucleotide, and ATP (disodium salt, Sonderqualität) were obtained from Boehringer (Mannheim, Germany). Apyrase VI and strophanthidin were purchased from Sigma (München, Germany), and 3-O-(1-(2-nitrophenyl)ethyl)ester ATP ("caged ATP") was purchased from Molecular Probes (Eugene, OR). NaCl (suprapure quality) and all other reagents (at least analytical grade) were from Merck (Darmstadt, Germany).

### Protein preparation

Na,K-ATPase was prepared from the outer medulla of rabbit kidneys using procedure C of Jørgensen (1974). This method yielded purified enzyme in the form of membrane fragments that consisted of flat sheets with a diameter of 0.2–1  $\mu\text{m}$  and contained  $\sim 0.8$  mg phospholipid and 0.2 mg cholesterol per milligram protein (Bühler et al., 1991). The specific ATPase activity was determined by the pyruvate kinase/lactate dehydrogenase assay (Schwartz et al., 1971). The protein concentration was determined by the Lowry method (Lowry et al., 1951), using bovine serum albumin as a standard. For all preparations the specific activity was in the range between 1900 and 2300  $\mu\text{mol P}_i$  per h and milligram protein at 37°C. The suspension of Na,K-ATPase-rich membrane fragments ( $\sim 3$  mg protein per ml) in buffer (25 mM imidazole sulfate, pH 7.5, 1 mM EDTA, 10 mg/ml sucrose) was frozen in samples of 100  $\mu\text{l}$ ; in this form the preparation could be stored for several months at  $-70^\circ\text{C}$  without significant loss of activity. Storage of thawed preparations at  $+4^\circ\text{C}$  did not affect the activity within a period of 4 weeks.

### Membrane experiments

Fast charge translocations in proteins of membrane preparations can be measured by the method of capacitive coupling. When the membrane fragments are adsorbed onto planar lipid bilayers and the ion transport activity is triggered in a synchronized manner, current transients will be observed in the external measuring circuit. This method was applied for example with purple membranes (Drachev et al., 1974; Bamberg et al., 1979) and Na,K-ATPase-containing membrane fragments (Fendler et al., 1985; Borlinghaus et al., 1987). In the case of bacteriorhodopsin, the transport is activated by light; in the case of the Na,K-ATPase, an ATP-concentration jump is performed by release of ATP from an inactive precursor, caged ATP (Kaplan et al., 1978; McCray et al., 1980). To obtain the pump current from the externally observed electric signals, a mathematical transformation has to be performed according to the equivalent circuit of the compound membrane system (Borlinghaus et al., 1987; Wuddel, 1994).

Planar lipid bilayers were formed from 1% diphytanoyl phosphatidylcholine in *n*-decane, as described previously (Borlinghaus et al., 1987). A Teflon cell was mounted in a Faraday cage in a thermostated aluminum block. The buffer composition was 30 mM imidazole, 10 mM  $\text{MgCl}_2$ , 1 mM EDTA, pH 7.2 (HCl), and specified concentrations of NaCl. If not mentioned otherwise, the temperature was 20°C. The potential across the bilayer was detected by Ag/AgCl electrodes, which were embedded in agar gel that was stained with black ink to shield the electrodes against stray-light artifacts. A membrane was formed across a hole of 1 mm diameter in the wall between the front (*trans*) and back (*cis*) compartment, and it was illuminated and observed through quartz windows in the *trans* compartment. Ultraviolet light from a flash bulb with known intensity profile passed a cutoff filter (Schott UG 11, 1 mm) and was focused on the membrane. The *cis* compartment, which had a volume of approximately 300  $\mu\text{l}$ , was equipped with a small magnetic stirrer. The buffer contained, if not indicated otherwise, 30 mM imidazole, 10 mM  $\text{MgCl}_2$ , 1 mM EDTA, 20 mM dithiothreitol, and the indicated amount of NaCl (pH 7.2). After a bilayer was formed, 250  $\mu\text{M}$  caged ATP, 0.4 U apyrase, and 50  $\mu\text{g/ml}$  membrane fragments were added to the *cis* side, followed by 1 min of smooth stirring. Membrane fragments adsorbed to the lipid bilayer with a time constant of several minutes. The properties of the compound membrane system were studied systematically. The kinetics of the measured signals under otherwise constant conditions depended neither on the number of adsorbed membrane fragments nor on the duration of the experiment. Only the signal amplitude, which is expected to be proportional to the number of capacitively coupled ion pumps, varied. It was shown previously that only fragments adsorbed with their extracellular phase to the bilayer contributed to the observed electric signals (Borlinghaus et al., 1987). The cleft between membrane fragments and lipid bilayer contained a limited aqueous volume with a restricted access to the bulk buffer phase (Borlinghaus et al., 1987; Wuddel, 1994). The specific access conductance

$G_p$  was typically  $2 \cdot 158 \cdot 10^{-7} \text{ s/cm}^2$ . The  $\text{Na}^+$  concentration in the cleft was determined to be 55–60% of the bulk phase (Wuddel, 1994).

The earliest experiments were performed 10 min after addition of the fragments. Typical lifetimes of the coupled membrane systems were 120 min. During this time the amplitude of the observed signals changed slowly, but their kinetics did not. Charge movements within the ion pumps in the membrane fragments could be detected as changes in the transmembrane electric voltage by the principle of capacitive coupling, as discussed previously (Borlinghaus et al., 1987; Wuddel, 1994). Voltage traces were detected by a voltage amplifier on the basis of an operational amplifier with an input impedance of  $10^{12} \Omega$  (Burr Brown 3528) and were recorded by a digital oscilloscope (Nicolet, model 4094A) upon the trigger of a 40- $\mu\text{s}$  UV flash or a charge pulse (Wuddel, 1994). Data were transferred to a personal computer for analysis.

### Charge-pulse induced relaxations

An electronic setup was used, as represented in Fig. 2, to charge up the membrane-protein system in a few microseconds. A pulse generator (Philips PM 5715, Rohde & Schwarz, Karlsruhe, Germany) generated a rectangular pulse of a length of 1–10  $\mu\text{s}$  with an amplitude of 1 V and charged up the membrane capacity via a transistor (2N918) implemented as a triode. In parallel to the membrane conductance, a shunt conductance of 57 G $\Omega$  as well as a short-circuit switch and an adjustable current source were connected to compensate for offset voltages. The *trans* electrode was

clamped to ground. Two different types of charge-pulse experiments were performed.

In the first type of experiment, charge pulse and light flash that induced an ATP concentration jump were triggered simultaneously. They were used to determine the voltage dependence of current transients induced by an ATP-concentration jump. As the time to charge up the membrane,  $t_C \approx 1 \mu\text{s}$ , was much faster than the release of ATP ( $\tau_{ATP} = 4.6 \text{ ms}$  at pH 7.2), the activation of the pump currents occurred in the presence of a membrane voltage. The time resolution of these experiments was limited by the kinetics of ATP release. The experiments were performed in a sequence, as shown in Fig. 3 A. The charge pulse protocol (charging up in 1  $\mu\text{s}$ , holding of the membrane voltage for 2 s, discharging in  $<1 \text{ ms}$ ) was performed three times with a recovery time of 60 s in between: twice without light flash, to produce reference signals, and the third time with the light flash. When there was no difference between the two reference signals, the difference between the third signal and reference 2 was collected as pump current-induced electric signal. Discharging the membrane after 2 s prolonged the life time of the membrane system significantly.

The second type of charge-pulse experiments was used to perform voltage-jump experiments (Fig. 3 B). Correspondingly, as in experiments of type 1, two reference signals were obtained in the absence of ATP; the ATP was then released by light flash. After a period of 4 s, when the pumps were in a quasi-stationary phosphorylated state, the voltage jump was applied by another charge pulse. In this type of experiment, the third signal was again evaluated when no difference was found between reference signals 1 and 2. The difference between the third signal and reference 2

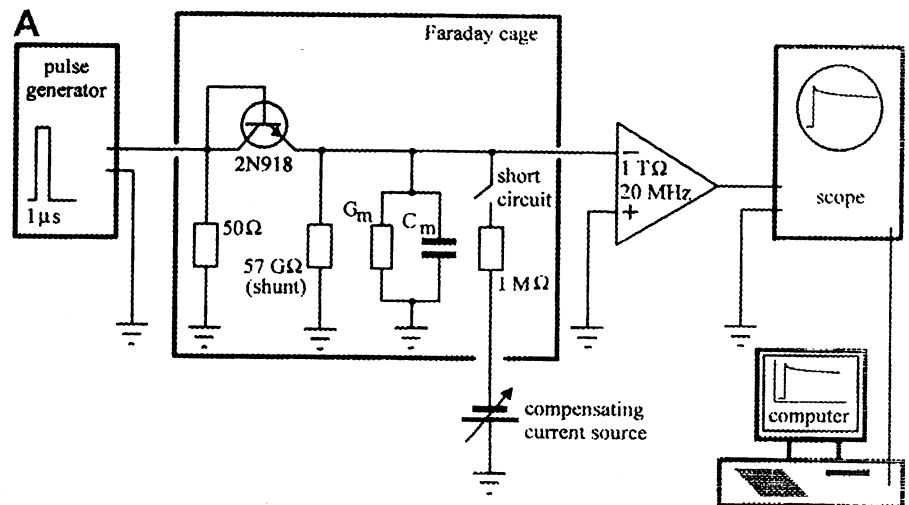
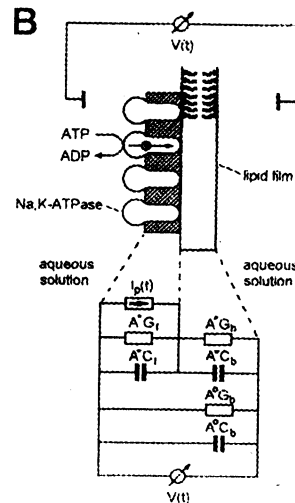


FIGURE 2 (A) Electronic setup of the charge-pulse experiments with capacitively coupled membrane fragments. The membrane system is simplified to a membrane capacitance,  $C_m$ , and membrane conductance,  $G_m$ . (B) The equivalent circuit of the compound membrane system consisting of a black lipid membrane with adsorbed Na,K-ATPase membrane fragments as discussed in a previous paper (adapted from Borlinghaus et al., 1987).



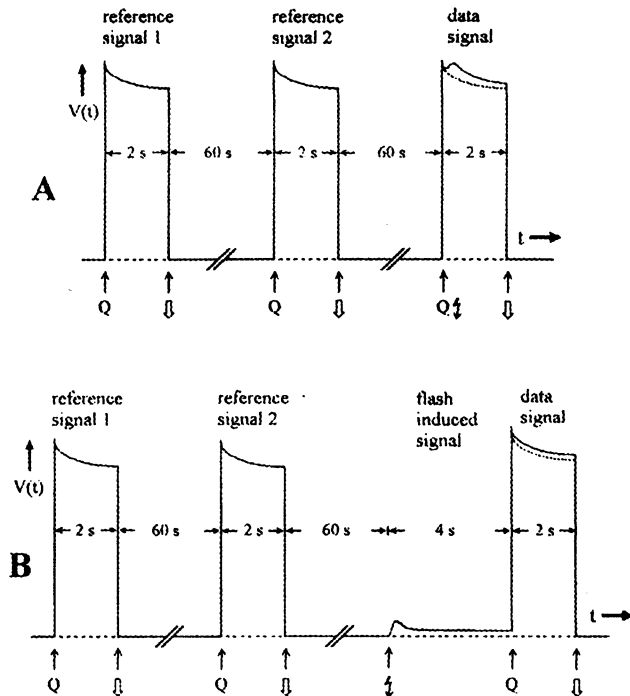


FIGURE 3 Experimental protocol of charge-pulse experiments with Na,K-ATPase-containing membrane fragments adsorbed to a lipid bilayer. The detected transmembrane voltage is shown as function of time. (A) Protocol to determine the voltage dependence of the transients induced by an ATP-concentration jump; (B) protocol to perform voltage-jump experiments with Na,K-ATPase molecules in a phosphorylated stationary state.  $Q$  refers to a voltage jump generated by a charge pulse, and the flash symbol indicates an ATP-concentration jump induced by a UV-light flash through the solution containing caged ATP. The symbol  $\cap$  indicates discharging of the membrane system by a 1 M $\Omega$  short circuit.

represented the voltage-induced charge movement between ATP-induced phosphorylated states.

Length and amplitude of the current pulse, which was used to charge up the membrane system, had to be chosen in a way so that the membrane voltage reached the desired voltage. The time constant was controlled by the capacity of the membrane system and serial resistance of electrodes and electrolyte. In the case of a 0.1-M electrolyte, we found  $\tau = 1.6 \text{ nF} \cdot 158 \cdot 200 \Omega = 0.32 \mu\text{s}$ . Therefore pulses with a duration of  $>1 \mu\text{s}$  maintained a defined membrane voltage. At the end of the current pulse, the total voltage was distributed according to the capacities of the membranes (Fig. 2 B):

$$U_f = U \cdot \frac{C_b}{C_f + C_b}; \quad U_b = U \cdot \frac{C_f}{C_f + C_b} \quad (1)$$

where  $U$ ,  $U_f$ , and  $U_b$  are the voltages generated by the charge pulse across the membrane system, the fragments, and the bilayer, respectively.  $C_f$  and  $C_b$  are the specific capacities of fragments and bilayer. The voltage drop across the membrane fragments can be estimated with the known capacitances  $C_f = 0.37 \mu\text{F}/\text{cm}^2$  and  $C_b = 1 \mu\text{F}/\text{cm}^2$  (Benz and Janko, 1976) to be

$$\frac{U_f}{U_f + U_b} = \frac{C_f}{C_b + C_f} = 0.27. \quad (2)$$

Membrane voltages of  $U = 150 \text{ mV}$ , which allowed the performance of experiments without a reasonable risk of breaking the membrane, thus produced an effective voltage of  $\sim 40 \text{ mV}$  across the Na,K-ATPase. The

voltages  $U_f$  and  $U_b$  dropped as a complex function of the capacities and the conductances across the membranes,  $G_f$  and  $G_b$ . Typical time constants obtained for the bilayer ( $\tau_b$ ) were 40 s and for the membrane fragments ( $\tau_f$ ) were 4.5 s (Wuddel, 1994). The consequence is that only the processes, which occur within the first 100 ms, can be assumed to be exposed to the full voltage ( $\Delta U_f \leq 5\%$ ). The sign of the voltage was defined as the potential of the *cis* relative to the *trans* compartment. With respect to the Na,K-ATPase in the membrane fragments adsorbed to the bilayer, the sign of the voltage corresponded to a cytoplasmic potential.

## RESULTS

In the absence of  $\text{K}^+$  ions and in the presence of  $\text{Na}^+$  concentrations  $>20 \text{ mM}$ , the reaction sequence of the Na,K-ATPase is confined to the scheme presented in Fig. 4. Upon addition of ATP (by release from the inert caged ATP), the enzyme is phosphorylated from its initial state  $\text{Na}_3\text{E}_1$  to  $(\text{Na}_3)\text{E}_1\text{-P}$  and subsequently undergoes a conformational transition into its other major conformation,  $\text{E}_2$ . As the return reaction into states of  $\text{E}_1$  (dashed lines in Fig. 4) is very slow, the distribution in the new stationary state depends on the (extracellular)  $\text{Na}^+$  concentration. In the presence of 20 mM  $\text{Na}^+$ , 95% of the enzyme will be in a phosphorylated state of  $\text{E}_2$  without a  $\text{Na}^+$  ion bound,  $\text{P-E}_2$ ; in the presence of 1 M  $\text{Na}^+$ , 85% of the pumps will remain in state  $(\text{Na}_3)\text{E}_1\text{-P}$ , as can be calculated with the model presented in the Appendix (Wuddel, 1994).

Effects of the cardiotonic steroid, strophanthidin, a specific inhibitor of the Na,K-ATPase, were investigated previously, whereby the reaction sequence  $(\text{Na}_3)\text{E}_1\text{-P} \rightarrow \text{P-E}_2(\text{Na}_2)$  was found to move three- to fourfold the amount of charge through the membrane dielectric as compared to the subsequent release of the other two  $\text{Na}^+$  ions,  $\text{P-E}_2(\text{Na}_2) \rightarrow \text{P-E}_2$  (Stürmer and Apell, 1992; Heyse et al., 1994). To obtain additional information on the dielectric coefficients of the whole reaction sequence,  $(\text{Na}_3)\text{E}_1\text{-P} \rightarrow \dots \rightarrow \text{P-E}_2$ ,

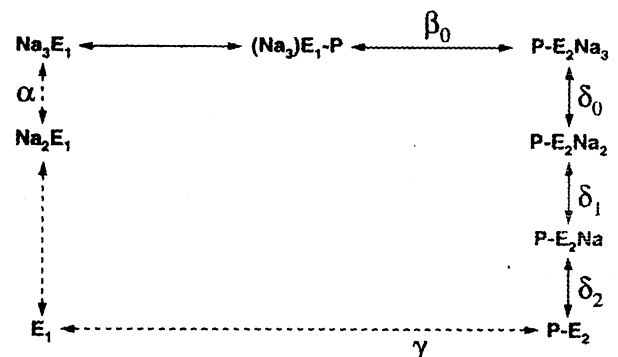


FIGURE 4 Reaction cycle of the Na,K-ATPase in the absence of  $\text{K}^+$  ions. The solid lines represent the reaction steps important for the initial current transient upon an ATP concentration-jump experiment. These partial reactions are fast compared with the return reactions from  $\text{P-E}_2$  to  $\text{Na}_3\text{E}_1$ . The existence of the dashed lines can be detected by the small steady-state component of the current signal at times longer than 1 s after the ATP jump.  $\alpha$ ,  $\beta$ ,  $\delta$ , and  $\gamma$  indicate the dielectric coefficients of the corresponding reaction steps and identify their electrogenicity.

charge-pulse experiments were performed according to these two different reaction types.

### Voltage dependence of the ATP-driven $\text{Na}^+$ transport

A charge-pulse experiment of type 1 was performed in standard buffer with 150 mM NaCl. Several ATP concentration-jump experiments were recorded in the absence of a charge pulse until the amplitude of the ATP-induced signal remained constant. Experiments were then performed in a sequence of different membrane voltages (0 mV,  $-150$  mV, 0 mV,  $+150$  mV, 0 mV), each in threefold repetition according to the protocol as described in the Materials and Methods section. Each set of three experiments was averaged to increase the signal/noise ratio. The intercalated experiments at 0 mV allowed controls for the time-dependent variation of the signal amplitude. The recorded voltage signals were transformed according to a published formalism into pump current signals (Borlinghaus and Apell, 1988). The result of a typical experiment is shown in Fig. 5 A. This series of experiments was performed many times with different membranes and protein preparations to confirm its reproducibility. In addition to 150 mM NaCl, these experiments were also carried out in 20 mM (Fig. 5 B), 500 mM, and 1000 mM NaCl (Fig. 5 C).

In the whole concentration range of  $\text{Na}^+$ , the maximum amplitude of the current transient was influenced by positive or negative membrane voltages. Positive membrane potentials always produced larger peak currents,  $I_{\text{peak}}$ , a larger total transferred charge,  $Q$ , (Fig. 6 A), and increased steady-state currents,  $I_{\infty}$  (Fig. 6 B). The rise time of the current transient did not depend significantly on the membrane potential but on the release kinetics of ATP from caged ATP (manuscript in preparation). Furthermore, the time constant characterizing the relaxation of the current transient,  $1/k_1$ , which could be assigned mainly to the conformational transition  $(\text{Na}_3)\text{E}_1\text{-P} \rightarrow \dots \rightarrow \text{P-E}_2(\text{Na}_3)$ , turned out to be hardly voltage sensitive (Fig. 6 C). These observations are in agreement with a transport of positive ions from the *cis* compartment toward the supporting bilayer and positive electrogenic coefficient in the reaction sequence.

### Voltage-dependent relaxations between phosphorylated states of $\text{E}_2$

Nakao and Gadsby (1986) performed voltage-induced current-relaxation experiments with the Na,K-ATPase. They detected strophanthidin-sensitive current transients upon voltage jumps from a resting potential of  $-40$  mV to voltages between  $-120$  mV and  $+80$  mV. This type of experiment could be repeated by charge-pulse experiments of the second type, in which ATP was released from its caged precursor and a voltage jump was applied across the membrane system after a steady state was reached. In this

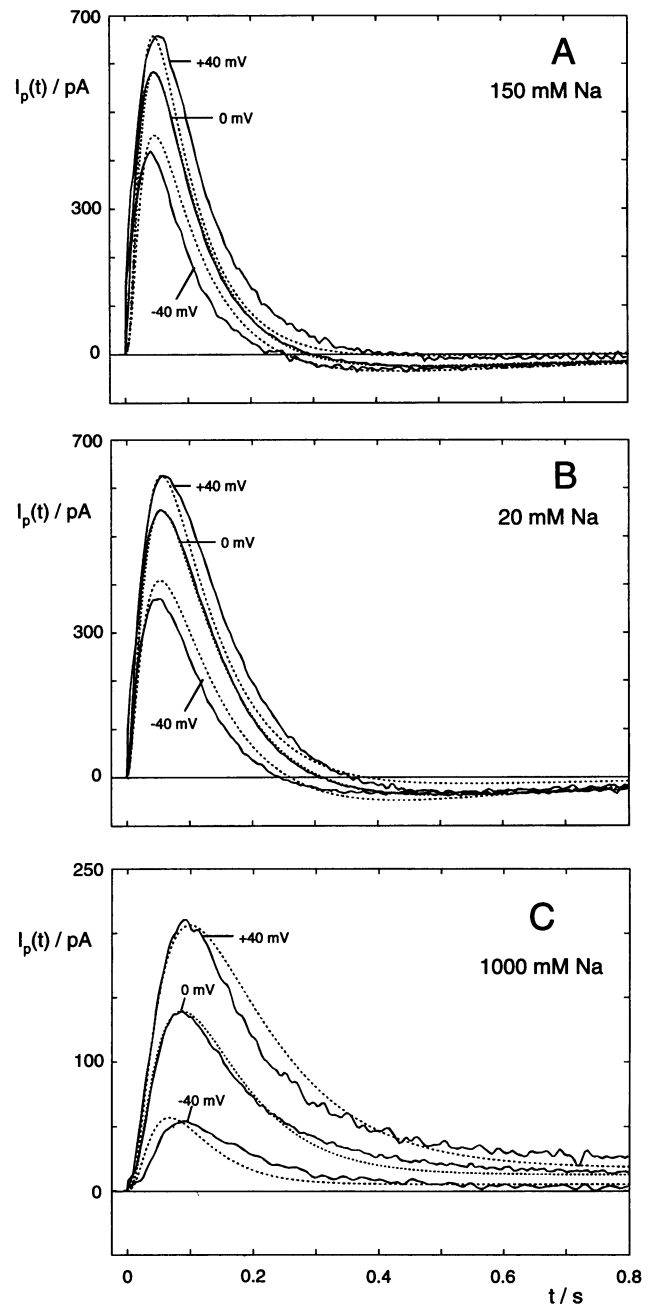


FIGURE 5 Pump-current transients after an ATP-concentration jump in buffer containing (A) 150 mM, (B) 20 mM, and (C) 1000 mM NaCl. ATP-induced enzyme phosphorylation initiated a subsequent current transient with membrane potential-dependent maximum amplitudes and kinetics. By using the charge-pulse method, the membranes could be charged up within  $1\text{--}2 \mu\text{s}$  at time  $t = 0$ . The voltages of  $\pm 150$  mV across the compound membrane (Fig. 2 B) corresponded to voltages of  $\pm 40$  mV across the Na,K-ATPase-containing membrane fragments. The current signals are averages over three successive experiments with the same membrane. The temperature was  $20^\circ\text{C}$ . The solid lines represent experimental data; the dotted lines are simulations, as explained in the Discussion section.

steady state there exists a dynamic equilibrium between the states  $(\text{Na}_3)\text{E}_1\text{-P} \leftrightarrow \text{P-E}_2(\text{Na}_3) \leftrightarrow \text{P-E}_2\text{Na}_2 \leftrightarrow \text{P-E}_2\text{Na} \leftrightarrow \text{P-E}_2$ . On the one hand, the distribution of the pumps between the states depends on the  $\text{Na}^+$  concentration. On the

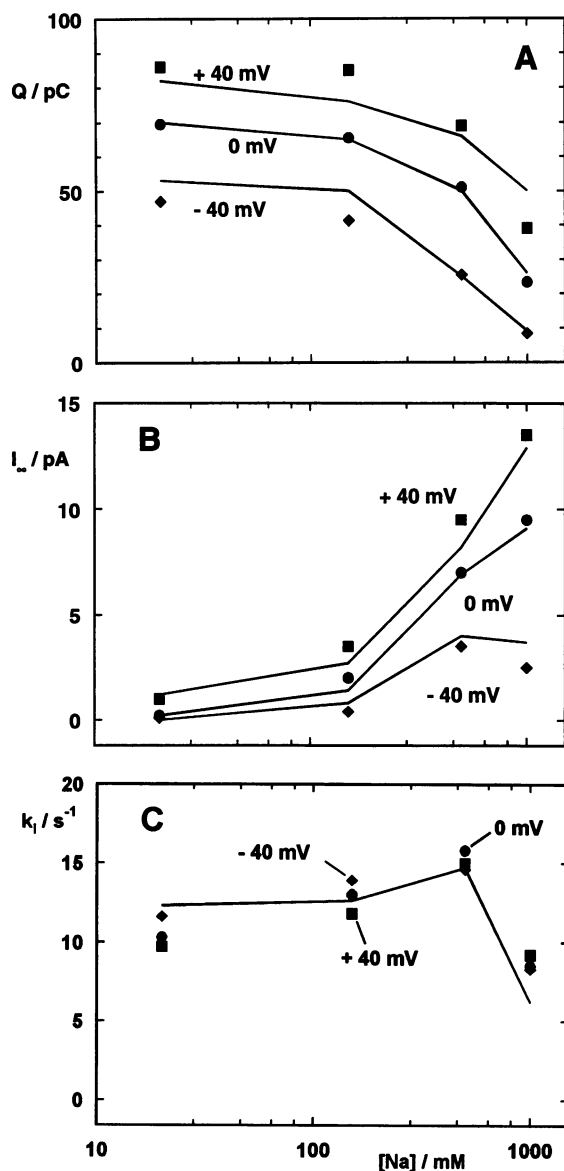


FIGURE 6 Analysis of the ATP concentration-jump experiments as shown in Fig. 5. The transferred charge,  $Q$ , the steady-state current,  $I_{\infty}$ , and the rate constant of the nearly monoexponential decay of the current transient,  $k_1$ , were taken as empirical parameters and plotted against membrane voltage and  $\text{Na}^+$  concentration. The voltage applied across the membrane system was  $\pm 150$  mV. The charge  $Q$  in panel A was determined as an integral of the current transient minus the steady-state current  $I_{\infty}$ . The lines are the result of simulations, as explained in the Discussion section. The theoretical values of  $Q$ ,  $I_{\infty}$ , and  $k_1$  were obtained from the simulated time course in the same way as from the experiments.

other hand, the reaction steps in this sequence are electrogenic and a voltage jump causes a relaxation into a new equilibrium, which can be detected by a transient current.

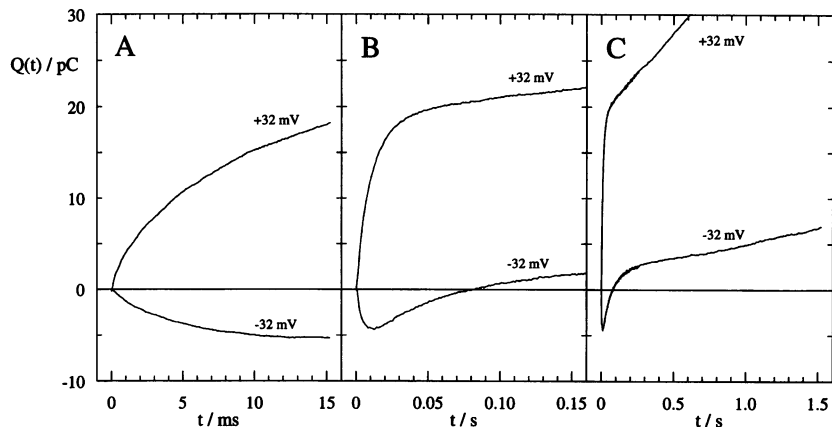
Because the detected voltage changes or the respective transient currents were small signals, extensive control experiments were performed to identify possible artifactual signal components. Voltage-jump experiments with pure

lipid membranes and with adsorbed membrane fragments in the absence of (caged) ATP showed a small initial voltage drop that was independent of the sign of the voltage jump and was completed in less than  $10 \mu\text{s}$ . Its origin lay in the lipid bilayer; however, the underlying mechanism could not be revealed. Inasmuch as it was identical for planar lipid bilayers in the absence and presence of adsorbed membrane fragments with pumps in the ATP-phosphorylated state and was faster than the time resolution of the setup, it was omitted before further analysis of the data.

Experiments were recorded in four time ranges between  $450 \mu\text{s}$  and  $1.5$  s in order to resolve different kinetic domains. The measured voltage transients were transformed to obtain the pump current signals,  $I_p(t)$ , which were integrated to obtain the (less noisy) amount of transported charge,  $Q(t)$ . One set of results, obtained at  $1$  M NaCl, is shown in Fig. 7. The externally applied voltage of  $120$  mV corresponded to a voltage of  $32$  mV across the Na,K-ATPase-containing membrane fragments. The fast components of the signal contained information about the extracellular  $\text{Na}^+$  release. The increase of charge in the time range  $>100$  ms (Fig. 7 C) is produced by the steady-state current of the pump,  $I_{\infty}$ , in the electrogenic Na-Na exchange mode of the pump (Glynn, 1985). It is clearly visible that  $I_{\infty}$  is voltage-dependent.  $I_{\infty}$  is smaller when the three  $\text{Na}^+$  ions in the first half-cycle are transferred against the membrane potential ( $-120$  mV) than with the membrane potential (Fig. 7C). The rebound of the charge trace for negative voltages during the time frame of  $10$ – $30$  ms was caused by turnovers subsequent to the voltage-jump induced relaxation process (Fig. 7 B). This complex behavior was qualitatively reproduced by numerical simulations of the proposed pump cycle (see below). As controls, these experiments were repeated in the absence of ATP. No significant charge movements could be detected (data not shown). Experiments with strophanthidin-inhibited enzyme could not be performed successfully because the membrane stability after addition of the ethanolic solution of the inhibitor decreased dramatically in charge-pulse experiments.

The fastest charge movements were assigned to the (electrogenic) ion-binding and release steps. The kinetics of these fast processes were investigated as a function of the  $\text{Na}^+$  concentration. In Fig. 8, the initial charge movement upon a voltage jump of  $\pm 120$  mV is represented as a function of the  $\text{Na}^+$  concentration. The sample rate was  $1$  per  $\mu\text{s}$ , and 3 to 10 voltage-jump experiments were averaged per trace in Fig. 8. The time course could be fitted by a single exponential,  $Q(t) = Q_{\text{max}} \cdot (1 - \exp(-k(V_m) \cdot t))$ . Examples of fits are included for experiments in the presence of  $150$  mM NaCl. Upon voltage jumps with positive potentials, which accelerate the forward rate constants of the pump cycle, the amount of charge,  $Q_{\text{max}}$ , increased monotonically with the  $\text{Na}^+$  concentration. In voltage-jump experiments with negative potentials  $|Q_{\text{max}}|$  decreased  $>500$  mM NaCl. The relaxation rate constants  $k(V_m)$  had values in the range between  $3500$   $\text{s}^{-1}$  and  $8000$   $\text{s}^{-1}$ . These numbers

FIGURE 7 Voltage jump-induced charge movements in ATP-phosphorylated Na,K-ATPase. The buffer contained 1 M NaCl. From originally recorded voltage signals, difference signals have been determined to obtain the pump-mediated component (see Materials and Methods section and Fig. 3 B). The voltage applied across the membrane system was  $\pm 120$  mV. The time-dependent amount of transferred charge,  $Q(t)$ , was calculated by transformation and integration. Data were recorded in three time ranges: 15 ms (A), 150 ms (B), and 1.5 s (C). In the shortest time range the dwell time between the data points was 30  $\mu$ s. The constantly increasing amount of charge in the time range  $>100$  ms is generated by steady-state turnover pumping of the Na,K-ATPase in its electrogenic Na-Na mode.



correspond to the rate constants of the dissociation of the second and third  $\text{Na}^+$  ion, as estimated by Heyse et al. (1994) from fluorescence experiments.

### Numerical simulations

The pump-current transients and derived quantities were simulated on the basis of two reaction models, one as introduced by Heyse et al. (1994) (Fig. 9 A), the other as shown in Fig. 9 B. The only difference between them is the introduction of state  $\text{P-E}_2(\text{Na}_3)$  in the second model. Because the experiments presented by Heyse et al. could be simulated completely by the simpler model (Fig. 9 A), we

applied this model first to the charge-pulse experiments presented in this paper. Even with major adjustments of the parameters published in Table V of Heyse et al. (1994), no consistent description of all voltage-jump experiments could be found. Specifically, the time course of current transients as shown in Fig. 5 could not be reproduced. Therefore we introduced an expanded pump cycle (Fig. 9 B) with the additional state,  $\text{P-E}_2(\text{Na}_3)$ , as proposed recently by Hilgemann (1994), which allowed the separation of the rate-limiting conformational change,  $(\text{Na}_3)\text{E}_1\text{-P} \rightarrow \text{P-E}_2(\text{Na}_3)$ , and a faster release of the first  $\text{Na}^+$  ion  $\text{P-E}_2(\text{Na}_3) \rightarrow \text{P-E}_2(\text{Na}_2)$  with a different electrogenicity. Details of the simulation procedure are given in the Appendix. A consistent description with an acceptable reproduction of all experiments could be performed with the expanded model by using the parameters published by Heyse et al. (1994) for the same source of protein. Modifications were introduced only because of the implementation of the additional state,  $\text{P-E}_2(\text{Na}_3)$ , and for the ion release steps on the extracellular side of the protein, which were not resolved before. The rate constants and dielectric coefficients of the electrogenic reaction steps of the pump cycle,  $\text{Na}_2\text{E}_1 \leftrightarrow \text{Na}_3\text{E}_1$  and  $(\text{Na}_3)\text{E}_1\text{-P} \leftrightarrow \text{P-E}_2(\text{Na}_3) \leftrightarrow \text{P-E}_2(\text{Na}_2) \leftrightarrow \text{P-E}_2(\text{Na}) \leftrightarrow \text{P-E}_2$ , (Fig. 9 B) are given in Table 1, as determined in the presented experiments. Examples of simulations are included in Figs. 5 and 6.

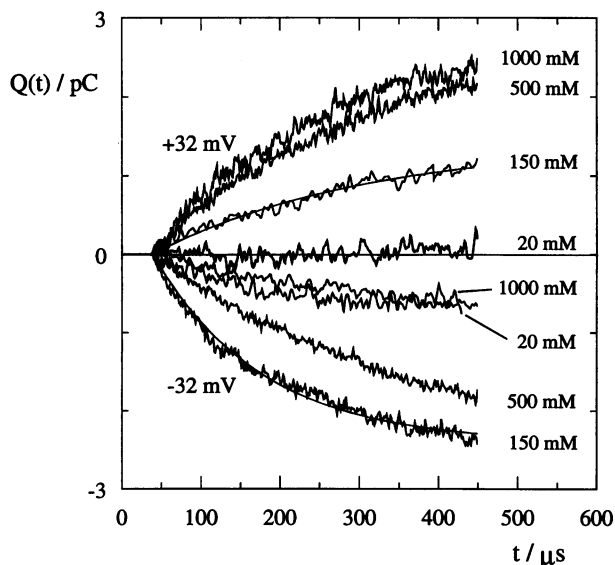


FIGURE 8 Charge relaxations induced by voltage-jump experiments in the presence of various  $\text{Na}^+$  concentrations with highest time resolution. Voltage jumps with positive potential produced a movement of  $\text{Na}^+$  ions in the forward direction with respect to the  $\text{Na}^+$  branch of the pump cycle ( $Q(t) > 0$ ). One hundred twenty millivolts applied externally corresponded to 32 mV across the pump-containing membranes. The smooth lines accompanying the 150 mM NaCl data represent fits of the data by the function  $Q(t, V_m) = Q_{\max} 158 (1 - \exp(-k(V_m) 158 t))$  with  $Q_{\max} (+150 \text{ mV}) = 1.42 \text{ pC}$ ,  $k (+150 \text{ mV}) = 3700 \text{ s}^{-1}$  and with  $Q_{\max} (-150 \text{ mV}) = -2.42 \text{ pC}$ ,  $k (-150 \text{ mV}) = 7300 \text{ s}^{-1}$ .

### DISCUSSION

In recent years, various protein preparations and experimental techniques have been used to analyze the electrogenicity of the Na,K-ATPase (Nakao and Gadsby, 1986, 1989; Lauger and Apell, 1988; Borlinghaus et al., 1987; Rakowski et al., 1991; Sturmer et al., 1991; Vasilets et al., 1991; Sturmer and Apell, 1992; Gadsby et al., 1993; Sagar and Rakowski, 1994; Hilgemann, 1994; Heyse et al., 1994). Although an agreement on a qualitative level can be found in the literature, the quantitative determination of dielectric coefficients and rate constants remained open, inasmuch as major contributions to the electrogenicity come from ion release (and binding) steps, which are very fast processes

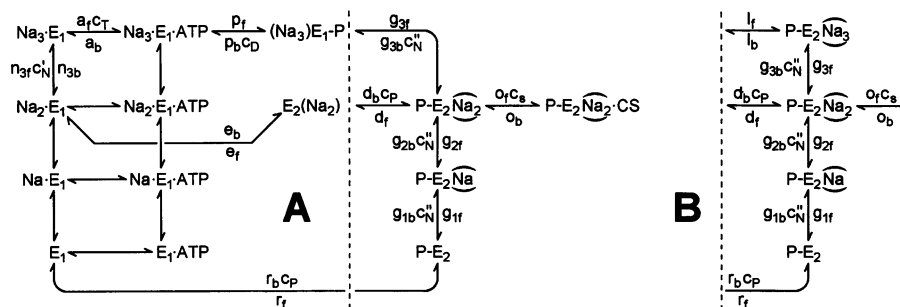


FIGURE 9 Kinetic reaction cycles of the  $\text{Na}^+$  transport in the  $\text{Na,K-ATPase}$ . Cycle A represents the cycle proposed by Heyse et al. (1994) in the absence of  $\text{K}^+$  ions. Cycle B, of which only the modified right part is shown, is expanded to include state  $\text{P-E}_2(\text{Na}_3)$ . The left part is identical to cycle A.  $a_f, p_f, \dots$  and  $a_b, p_b, \dots$  are the rate constants in forward and backward direction, respectively.  $c_T, c_D,$  and  $c_P,$  represent the concentrations of ATP, ADP, and  $\text{P}_i$ .  $c_N^i$  and  $c_N^e$  are the sodium concentrations on the cytoplasmic and extracellular side of the membrane. Transitions without corresponding rate constants were assumed to be fast compared with the other reaction steps and were treated as being permanently in equilibrium with an equilibrium constant taken from literature. The state  $\text{P-E}_2(\text{Na}_2)\text{-CS}$  was included to account for inhibition experiments with cardiac steroids (CS).  $c_s$  stands for the concentration of strophanthidin, if applied.

compared with other partial reactions of the pump cycle. So far, the only kinetic analysis of the reaction sequence  $(\text{Na}_3)\text{E}_1\text{-P} \leftrightarrow \text{P-E}_2(\text{Na}_3) \leftrightarrow \text{P-E}_2(\text{Na}_2) \leftrightarrow \text{P-E}_2(\text{Na}) \leftrightarrow \text{P-E}_2$  has been published by Hilgemann (1994), who applied the giant patch method at  $37^\circ\text{C}$  to membranes containing  $\text{Na,K-ATPase}$  from guinea pig myocytes. The forward rate constant of the conformational transition to state  $\text{P-E}_2(\text{Na}_3)$ , corresponding to  $l_f$ , was determined to be  $640 \text{ s}^{-1}$ , and the equilibrium constant (corresponding to  $K_1$ ) was 0.03. Hilgemann assumed a rapid release of one  $\text{Na}^+$  ion, another (electroneutral) conformational rearrangement to reach state  $\text{P-E}_2(\text{Na}_2)$ , with a forward rate constant of  $40,000 \text{ s}^{-1}$  and an equilibrium constant of 10, and finally a subsequent (instantaneous) release of two  $\text{Na}^+$  ions. In his experiments, the dielectric constant of the first resolved reaction step was 0.74 and of the second step, 0.26. These numbers are in

good agreement with those of Heyse et al. (1994) and the findings in this presentation.

The introduction of the charge-pulse technique to adsorbed membrane fragments containing  $\text{Na,K-ATPase}$  allowed an increase of the time resolution compared with ATP concentration-jump experiments from  $\sim 5 \text{ ms}$  to  $> 1 \mu\text{s}$ . An additional advantage of this method was that it selectively addressed electrogenic reactions of the  $\text{Na,K-ATPase}$ . A disadvantage was the complex analysis of the coupled bilayer and membrane-fragment system. In addition to the mathematical formalism, a determination of the parameters  $G_f$  and  $G_b$  was necessary for quantitative analyses (Fig. 2 B). In addition, current components of the passive membrane system, which were induced by the charge-pulse, were detected and had to be subtracted to obtain the pump-induced contributions (Fig. 3).

TABLE 1 Kinetic and dielectric parameters of the electrogenic reaction steps in the  $\text{Na}$ -only mode of the  $\text{Na,K-ATPase}$

Reaction	Parameter	Value	Range of confidence	Dielectric constant	Notes
$\text{Na}_2\text{E}_1 \leftrightarrow \text{Na}_3\text{E}_1$	$n_{3f}$	$2 \cdot 10^5 \text{ M}^{-1} \text{ s}^{-1}$	$\pm 50\%$	$\alpha = 0.25$	*
	$K_{n3}$	4 mM	$\pm 10\%$	$\alpha = 0.25$	*
$(\text{Na}_3)\text{E}_1\text{-P} \leftrightarrow \text{P-E}_2(\text{Na}_3)$	$l_f$	$25 \text{ s}^{-1}$	$\pm 5\%$	$\beta_0 = 0.1$	†
	$K_1$	$\approx 0.1$	$0.1 \leq K_1 \leq 5$	$\beta_0 = 0.1$	
$\text{P-E}_2(\text{Na}_3) \leftrightarrow \text{P-E}_2(\text{Na}_2)$	$g_{3f}$	$1400 \text{ s}^{-1}$	$\pm 5\%$	$\delta_0 = 0.65$	
	$K_{g3}$	0.1 M	$\pm 10\%$	$\delta_0 = 0.65$	
$\text{P-E}_2(\text{Na}_2) \leftrightarrow \text{P-E}_2(\text{Na})$	$g_{2f}$	$700 \text{ s}^{-1}$	$\pm 5\%$	$\delta_1 = 0.1\text{--}0.2$	
	$K_{g2}$	1.5 M	$\pm 10\%$	$\delta_1 = 0.1\text{--}0.2$	
$\text{P-E}_2(\text{Na}) \leftrightarrow \text{P-E}_2$	$g_{1f}$	$4000 \text{ s}^{-1}$	$\pm 5\%$	$\delta_2 = 0.1\text{--}0.2$	
	$K_{g1}$	0.09 M	$\pm 10\%$	$\delta_2 = 0.1\text{--}0.2$	

The rate constants ( $n_{3f}, l_f, g_{3f}, g_{2f}, g_{1f}$ ) and equilibrium constants ( $K_{n3}, K_1, K_{g3}, K_{2f}, K_{1f}$ ) were determined at  $T = 20^\circ\text{C}$ . These numbers were used in all numerical simulations presented in this paper, according to the pump cycle of Fig. 9 B.

\* Binding of the third  $\text{Na}^+$  ion to the cytoplasmic side could not be analyzed by the presented experimental method. The applied values were taken from Heyse et al. (1994).  $\alpha = 0.25$  fulfills well the boundary condition that one  $\text{Na}^+$  ion is transported in the electrogenic  $\text{Na}/\text{Na}$ -exchange mode.

† Because of the low electrogenicity of the conformational change, a rather wide range of the equilibrium constant,  $K_1$ , was found in different experiments. Although the forward rate constant,  $l_f$ , as the rate-limiting step could be determined accurately, most experiments were not significantly sensitive to the back reaction rate,  $l_b$ . With  $K_1 = 0.1$ , a consistent description of all experiments was possible.

Another principal problem in understanding the electrogenicity consists in the complexity of the pump itself. Even in the Na-only mode, at least 11 reaction steps can be identified (see Appendix), partly electrogenic and partly electroneutral, and it is not possible to confine the externally triggered pump action to a single step. A certain selection of partial reaction is possible by variation of the  $\text{Na}^+$  concentration and adjustment of the time range in which observations were made. The strategy was to describe the experimental observations with as simple a model as possible. To determine the contributions of the different electrogenic reaction steps, we used the analysis-by-model simulations according to Fig. 9 B, with the restriction that one set of parameters had to fit all (or most) of the experiments. Such a set was found on the basis of the numbers published recently (Heyse et al., 1994), with the modifications and extensions given in Table 1. A crucial concern is the uniqueness of the determined set of parameters. Arguments for the reliability of the procedure and the parameters are the following: 1) Many of the parameters known from the literature are determined by different approaches. They were fixed to the known values or modified only slightly. 2) The influence of single parameters on shape or amplitude of experimental signals is usually very specific, and the possibilities of other parameters to compensate this effect are only limited. 3) The set of parameters was built up iteratively. Each set of new experiments, which had to be modeled by the simulation procedure, could introduce only modifications that conserved the reproduction of earlier experiments. 4) For each parameter a range of confidence was introduced, which indicates the uncertainty of the "fit."

### Kinetic and dielectric characterization of the $\text{Na}^+$ translocation

In its  $\text{E}_1$  conformation the Na,K-ATPase can bind three  $\text{Na}^+$  ions from the cytoplasmic side. Two ions are bound to negatively charged sites that are placed in the electric surface of the protein. These sites are assumed to be the same to which  $\text{K}^+$  ions also bind (Läuger, 1991). From experiments with the voltage-sensitive fluorescence dye RH 421, it has been interpreted to mean that binding of one  $\text{Na}^+$  to the third uncharged site is electrogenic (Heyse et al., 1994, Schulz and Apell, 1995). The charge-pulse relaxation method applied in this paper allowed an estimation in agreement with the fluorescence experiments that the binding process is fast ( $n_{3f} \geq 10^6 \text{ M}^{-1} \text{ s}^{-1}$ ) and electrogenic ( $\alpha \leq 0.25$ ). ATP binding and phosphorylation of the enzyme,  $\text{Na}_3\text{E}_1 \rightarrow \text{Na}_3\text{E}_1\text{ATP} \rightarrow (\text{Na}_3)\text{E}_1\text{-P}$ , are electroneutral steps and were accounted for with parameters comparable to those published recently (Heyse et al., 1994):  $a_f = 3.5 \cdot 10^6 \text{ M}^{-1} \text{ s}^{-1}$ ,  $a_b = 0.4 \text{ s}^{-1}$ ,  $p_f = 200 \text{ s}^{-1}$ ). Estimations of the dielectric coefficients of this reaction sequence resulted in an upper limit of 0.07 by charge-pulse experiments of type 1 at 2 M NaCl. At this high  $\text{Na}^+$  concen-

tration, the enzyme is trapped almost quantitatively in state  $(\text{Na}_3)\text{E}_1\text{-P}$ . Borlinghaus et al. (1987) found zero electrogenicity in experiments with  $\alpha$ -chymotrypsin-treated enzyme.

### Rate-limiting conformational change and release of the first $\text{Na}^+$ ion are distinct steps

From the literature it is known that the transition  $(\text{Na}_3)\text{E}_1\text{-P} \rightarrow \text{P-E}_2$  contains the rate-limiting and major charge-translocating step (Forbush, 1984; Läuger et al., 1991; Heyse et al., 1994). Utilizing the specific action of the inhibitor strophanthidin, Stürmer and Apell (1992) found evidence for at least two electrogenic partial reactions,  $(\text{Na}_3)\text{E}_1\text{-P} \rightarrow \text{P-E}_2\text{Na}_2$  and  $\text{P-E}_2\text{Na}_2 \rightarrow \text{P-E}_2$ . Experiments in which the amount of transferred charge was measured in the presence and absence of strophanthidin allowed the determination of the corresponding dielectric coefficients, 0.75 for  $(\text{Na}_3)\text{E}_1\text{-P} \rightarrow \text{P-E}_2(\text{Na}_2)$  and 0.2–0.4 for  $\text{P-E}_2(\text{Na}_2) \rightarrow \text{P-E}_2$  (Heyse et al., 1994).

By charge-pulse experiments, the kinetics of pump-current transient could be measured and analyzed as a function of the membrane potential (Figs. 5–8). A simulation of these experiments with the simpler model of Fig. 9 A, in which the rate-limiting and major electrogenic reaction step are the same, failed to reproduce the time-resolved measurements. The following experimental findings were in contradiction to the assumption that the major electrogenic step is rate-limiting.

1. In the presence of  $\text{Na}^+$  concentrations  $>1 \text{ M}$ , the amplitude of the pump-current transient was increased after the addition of strophanthidin (Wuddel et al., 1994), as shown in Fig. 10. A simulation of the transients in the presence of inhibitor was not possible under the assumption that the electrogenic step was rate-limiting (simulation 2 in Fig. 10). Introduction of the reaction  $(\text{Na}_3)\text{E}_1\text{-P} \rightarrow \text{P-E}_2(\text{Na}_3)$  as a rate-limiting step with an equilibrium constant  $K_1 = 0.1$  and low electrogenicity followed by a fast step with a large charge movement allowed a qualitative reproduction of the experimental observation (simulation 3 in Fig. 10).

2. The relaxation rate  $k_1$  of the ATP-induced current transients, which was mainly controlled by the rate-limiting process, showed no significant voltage dependence (Fig. 6 C). This observation cannot be reproduced by the simpler model of Fig. 9 A, in which the rate-limiting step has a dielectric coefficient of 0.75.

3. The voltage-induced current transients, which were measured at high time resolution (Fig. 8), had relaxation rates of the same order of magnitude ( $3500 \text{ s}^{-1}$ – $8000 \text{ s}^{-1}$ ) over the whole concentration range between 20 mM and 1 M. In this range the release of each of the three  $\text{Na}^+$  ions was covered by appropriate concentrations, and all ions were released quickly. In the simpler model (Fig. 9 A), the release of the "first" ion would be included in the rate-limiting step. Under this condition the fast ion release could not be reproduced in the presence of  $\text{Na}^+ >500 \text{ mM}$ .

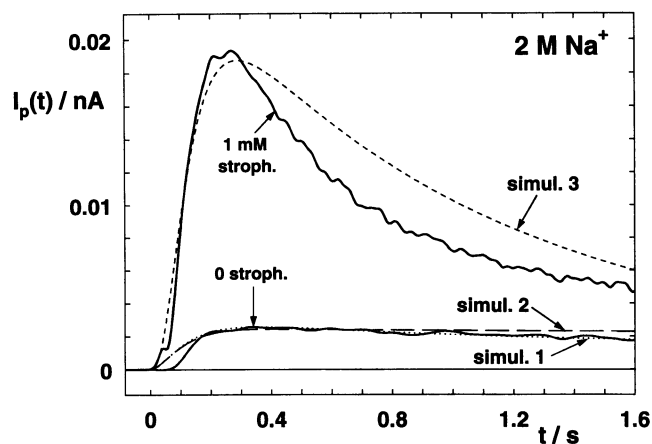


FIGURE 10 Pump-current transient induced by an ATP concentration jump in the presence and absence of the specific inhibitor strophantidin (stroph.) in the buffer containing 2 M NaCl. In the absence of the inhibitor, only a small transient could be found. After addition of 1 mM strophantidin, a significant increase was observed, caused by the inhibitor-induced continuation of the reaction  $(\text{Na}_3)\text{E}_1\text{-P} \rightarrow [\text{P-E}_2(\text{Na}_3) \rightarrow \text{P-E}_2(\text{Na}_2) \rightarrow \text{P-E}_2(\text{Na}_2)_{\text{stroph.}}$ , which contained the major electrogenic step (Wuddel et al., 1994). Simulations were performed for several conditions in the absence of stroph. (simul. 1), in which no discrimination was observed between both models of Fig. 9. In the presence of strophantidin, simulations were different for both models: simul. 2 according to the model of Fig. 9 A and simul. 3 according to Fig. 9 B.

Both models of Fig. 9 were also applied to results of the voltage-jump experiments, with cardiac myocytes performed by Nakao and Gadsby (1986). To simulate their experiments, the rate constants had to be adapted to the temperature of 36°C. We accounted for this elevated temperature by multiplying all rate constants by a factor of 5 (which corresponds to an average activation energy of 75 kJ/mol). In Fig. 11 the original data of the voltage-dependent charge movement and relaxation behavior were compared with simulations of both models. Although the transferred charge,  $Q$ , was similarly well reproduced by both models, the relaxation rate constant,  $k$ , could be described only by the extended reaction sequence of Fig. 9 B,  $(\text{Na}_3)\text{E}_1\text{-P} \leftrightarrow \text{P-E}_2(\text{Na}_3) \leftrightarrow \text{P-E}_2(\text{Na}_2) \leftrightarrow \text{P-E}_2(\text{Na}) \leftrightarrow \text{P-E}_2$ . The voltage independence of the relaxation rate for holding potentials  $V > 0$  could be obtained only by  $K_1 = 0.1$  and  $\beta_0 < 0.1$ .

All of these findings corroborate the extended reaction sequence of Fig. 9 B as the adequate model for the sodium pathway of the Na,K-ATPase.

#### Release of the second and third $\text{Na}^+$ ion on the extracellular side

By making use of the specific action of strophantidin, Heyse et al. (1994) were able to separate the dielectric properties of the partial reactions  $(\text{Na}_3)\text{E}_1\text{-P} \leftrightarrow \text{P-E}_2(\text{Na}_2)$  and  $\text{P-E}_2(\text{Na}_2) \leftrightarrow \text{P-E}_2$ . For release of the second and third  $\text{Na}^+$  ion they determined dielectric coefficients  $\delta_1 = \delta_2 =$

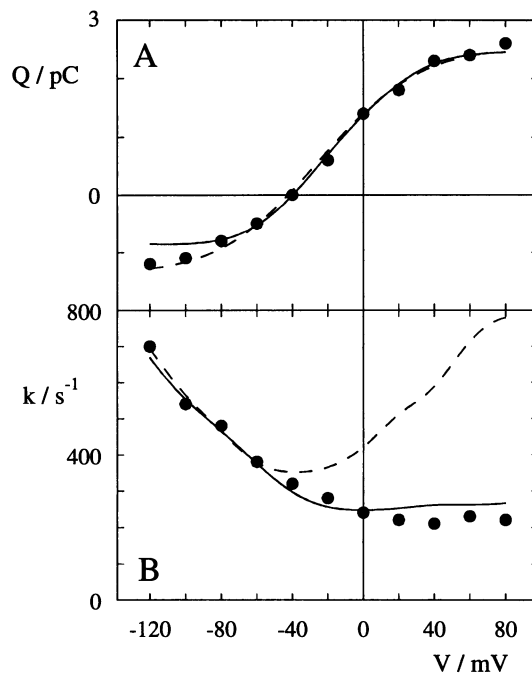


FIGURE 11 Voltage-dependent parameters of transient Na,K-pump currents. Currents were induced by voltage jumps to the indicated holding potential from a resting potential of  $-40$  mV. (A) Total translocated charge,  $Q$ , and (B) reciprocal relaxation time,  $k$ , of the current transient as a function of the voltage. Data points were obtained from whole-cell clamp experiments with cardiac myocytes by Nakao and Gadsby (1986). The lines represent numerical simulations with the two different models of Fig. 9 A, in which the rate-limiting and major charge-translocating steps were the same, (dashed line) and of Fig. 9 B, in which the rate-limiting conformational change and the fast and mainly electrogenic release of the first  $\text{Na}^+$  ion were separated (solid line).

0.1. These numbers were confirmed in the framework of this study (Table 1).

Charge-pulse experiments of type 2 could be used to determine voltage jump-induced charge movements in the Na,K-ATPase. This technique was used to analyze the kinetics of the  $\text{Na}^+$  release (Figs. 7 and 8). At highest time resolution, relaxation rates were obtained between  $3500 \text{ s}^{-1}$  and  $8000 \text{ s}^{-1}$ . The best fitting simulations resulted in rate constants of  $g_{3f} = 1400 \text{ s}^{-1}$ ,  $g_{2f} = 700 \text{ s}^{-1}$ , and  $g_{1f} = 4000 \text{ s}^{-1}$  at zero voltage and dielectric coefficients of  $\delta_0 = 0.65$ ,  $\delta_1 = 0.1\text{--}0.2$ , and  $\delta_2 = 0.1\text{--}0.2$ . The corresponding equilibrium dissociation constants (Table 1) were in good agreement with the findings of Heyse et al. (1994). In their work, the  $\text{Na}^+$ -release rates could be estimated only indirectly by  $\text{K}^+$ -strophantidin antagonism experiments, and the rates were proposed to be  $\geq 5000 \text{ s}^{-1}$ . The discrepancy may be explained by their indirect reasoning.

The decreasing relaxation amplitude for  $\text{Na}^+$  concentrations  $>150$  mM for negative voltage jumps can be attributed to increasing occupancy of state  $\text{P-E}_2(\text{Na}_3)$  with rising  $\text{Na}^+$  concentrations, as has been checked by numerical simulations. Because of the fact that the reaction step  $\text{P-E}_2(\text{Na}_3) \rightarrow (\text{Na}_3)\text{E}_1\text{-P}$  is only slightly electrogenic, pump molecules, which are in state  $\text{P-E}_2(\text{Na}_3)$  before the voltage

jump, will no longer contribute significantly to the relaxation current.

### Refined electrostatic model of the Na,K-ATPase

By comparison of the numerical simulations of the extended pump cycle in Fig. 9 B with all of the available experiments, an electrostatic model of the Na,K-ATPase can be proposed on the basis of the Post-Albers cycle, as shown in Fig. 12. This model is evolved from a recently published one (Heyse et al., 1994) and characterizes the kinetic and dielectric properties of the Na,K-pump known so far.

1. In its  $E_1$  state, the enzyme is able to bind two cations ( $\text{Na}^+$  or  $\text{K}^+$ ) to two negatively charged binding sites, which are placed in the (dielectric) surface of the protein. The third site is highly specific for  $\text{Na}^+$  and is uncharged. Binding to this site is electrogenic ( $\alpha = 0.25$ ). This property is a strong indication for its placement within the protein dielectric. ATP binding, enzyme phosphorylation, and ion occlusion are electroneutral steps (Borlinghaus et al. 1987). The latter effect can be explained by the idea that only a kind of gate is closed in front of the ion-binding sites.

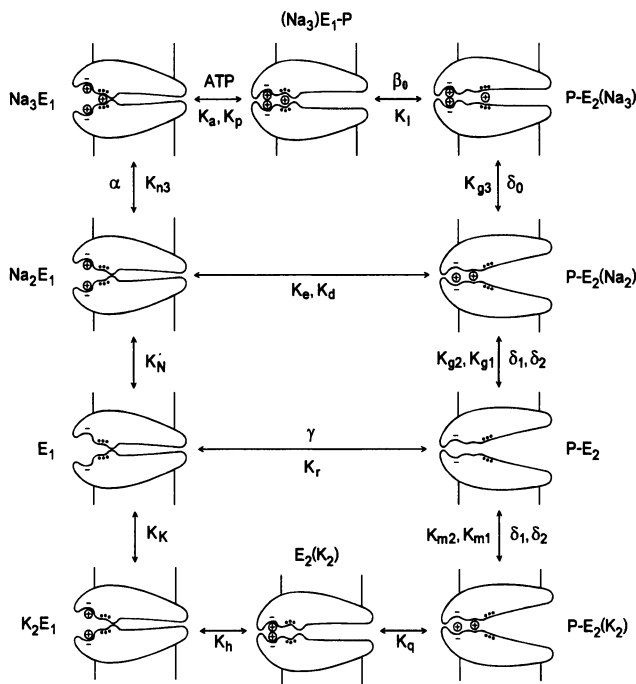


FIGURE 12 Electrostatic model of the Na,K-ATPase on the basis of a detailed determination of the dielectric coefficients for all reaction steps. The reactions accompanied by  $\alpha$ ,  $\beta$ ,  $\delta$ , and  $\gamma$  are electrogenic (cf. Table 1). In the  $E_1$  conformation of the pump, two negatively charged binding sites are presented in the dielectric surface of the protein, and one uncharged,  $\text{Na}^+$ -specific site is placed within the protein dielectric. In the  $E_2$  conformation, all binding sites are accessible only through an access channel, which has a dielectric depth depending on the occupation of the binding sites (see Discussion section). We would like to note that the drawing is meant only schematically and does not contain any structural concepts.

2. The subsequent conformational change is slow and of low electrogenicity ( $\beta_0 = 0.1$ ). Therefore the  $\text{Na}^+$  ion bound to the neutral binding site can be hardly moved perpendicular to the plane of membrane.

3. The major electrogenic process is the fast release of the first  $\text{Na}^+$  ion to the extracellular side ( $\delta_0 = 0.65$ ), most probably from the neutral site (Heyse et al., 1994). The other two  $\text{Na}^+$  ions are also released with high rate constants, although with small dielectric coefficients ( $\delta_1 = \delta_2 = 0.1-0.2$ ). If it is assumed that the charged binding sites are placed behind the site of the first ion with respect to the external side, the lower dielectric coefficients can be explained by a protein relaxation correlated with (or following after) the release of the first  $\text{Na}^+$  ion. A possible mechanism could be a widening of the access channel between the aqueous phase and the binding sites. This does not necessarily mean that a structure exists comparable to known ion channels and that the access structure is increased in diameter as is suggested in Fig. 12. A diffusion of water molecules into the protein structure would be sufficient to shift the dielectric surface of the protein (and the equipotential lines) to the binding sites. The intruding water molecules would also facilitate (re-)hydration of the ions. (The process de-/rehydrating the ions has not been considered at all in the whole transport process.)

4. The mentioned protein relaxation could also account for the altered ion selectivity of the binding sites on the extracellular side, which promotes binding of two  $\text{K}^+$  ions. This process is electrogenic (Rakowski et al., 1991), with dielectric coefficients comparable to that of binding of the second and third  $\text{Na}^+$  ion,  $\delta_1 = \delta_2 = 0.1-0.2$  (Heyse et al., 1994). The following reaction steps to reach state  $\text{K}_2\text{E}_1$  are electroneutral, as both cations are paired with the oppositely charged binding sites and the release to the cytoplasmic site is electroneutral because of the finding that the sites are now placed again in the dielectric surface of the protein.

5. Finally, in the electrogenic Na/Na-exchange mode in the presence of extracellular  $\text{Na}^+$ , the backward-directed movement of  $\text{Na}^+$ ,  $\text{P-E}_2(\text{Na}_2) \rightarrow \text{Na}_2\text{E}_1$  is electroneutral, as  $\text{Na}^+$  can be taken as congener of  $\text{K}^+$ , and in the absence of extracellular  $\text{Na}^+$ , an uncoupled  $\text{Na}^+$  transport may occur. In this case the back reaction,  $\text{P-E}_2 \rightarrow \text{E}_1$ , would be strongly electrogenic with a dielectric coefficient,  $\gamma$ , which can be calculated from the stoichiometry of the transport cycle:  $\alpha + \beta_0 + \delta_0 + \gamma = 3$ . With the above-mentioned values,  $\gamma = 1.8$  was obtained. The electrogenicity of this process, although it would be very strong, cannot be investigated with our presented methods.

We are grateful to Milena Roudna for excellent technical assistance and to Dr. Werner Stürmer for helpful discussions. Data presented in this publication are part of the Ph.D. thesis of Ingo Wuddel.

This work was supported by the Deutsche Forschungsgemeinschaft (Sonderforschungsbereich 156).

## APPENDIX

## Numerical analysis of the transient pump current

To simulate the ion pump-mediated current transients, a mathematical model was formulated on the basis of the reaction scheme of Fig. 9 B. To perform numerical analyses on a personal computer, FORTRAN programs were written according to the following definitions.

If  $x[A]$  is the mole fraction of pump molecules in state A, the reaction cycle of Fig. 9 B may be formalized by a series of variables:

$$\begin{aligned}
 x_1 &= x[\text{Na}_2\text{E}_1] + x[\text{NaE}_1] + x[\text{E}_1] \\
 x_2 &= x[\text{Na}_3\text{E}_1] \\
 x_3 &= x[\text{Na}_2\text{E}_1\text{ATP}] + x[\text{NaE}_1\text{ATP}] + x[\text{E}_1\text{ATP}] \\
 x_4 &= x[\text{Na}_3\text{E}_1\text{ATP}] \\
 x_5 &= x[(\text{Na}_3)\text{E}_1\text{-P}] \\
 x_6 &= x[\text{P-E}_2(\text{Na}_3)] \\
 x_7 &= x[\text{P-E}_2(\text{Na}_2)] \\
 x_8 &= x[\text{P-E}_2(\text{Na})] \\
 x_9 &= x[\text{P-E}_2] \\
 x_{10} &= x[\text{E}_2(\text{Na}_2)] \\
 x_{11} &= x[\text{P-E}_2(\text{Na}_2)\text{-CS}]
 \end{aligned} \tag{A1}$$

With following relations:

$$\begin{aligned}
 x[\text{Na}_2 \cdot \text{E}_1] &= x_1 \cdot \frac{n_1 \cdot n_2}{P} \\
 x[\text{Na}_2 \cdot \text{E}_1 \cdot \text{ATP}] &= x_3 \cdot \frac{n_1 \cdot n_2}{P} \\
 n_i &= \frac{c'_{N,i}}{K'_{N,i}} = \frac{x[\text{Na}_i \cdot \text{E}_1]}{x[\text{Na}_{i-1} \cdot \text{E}_1]} = \frac{x[\text{Na}_i \cdot \text{E}_1 \cdot \text{ATP}]}{x[\text{Na}_{i-1} \cdot \text{E}_1 \cdot \text{ATP}]}, \\
 & \quad i = 1, 2
 \end{aligned}$$

$$P = 1 + n_1 + n_1 \cdot n_2$$

the reaction cycle is represented by 11 coupled differential equations

$$\begin{aligned}
 \dot{x}_1 &= - \left[ a_f \cdot c_T + \frac{n_1 \cdot n_2}{P} (n_{3f} \cdot c'_N + e_b) + r_b \cdot c_P \cdot \frac{1}{P} \right] x_1 \\
 & \quad + n_{3b} \cdot x_2 + a_b \cdot x_3 + r_f \cdot x_8 + e_f \cdot x_9 \\
 \dot{x}_2 &= n_{3f} \cdot c'_N \cdot \frac{n_1 \cdot n_2}{P} x_1 - [n_{3b} + a_f \cdot c_T] \cdot x_2 + a_b \cdot x_4 \\
 \dot{x}_3 &= a_f \cdot c_T \cdot x_1 - \left[ a_b + n_{3f} \cdot c'_N \cdot \frac{n_1 \cdot n_2}{P} \right] x_3 + n_{3b} \cdot x_4 \\
 \dot{x}_4 &= a_f \cdot c_T \cdot x_2 + n_{3f} \cdot c'_N \cdot \frac{n_1 \cdot n_2}{P} \cdot x_3 \\
 & \quad - [a_b + n_{3b} + p_f] x_4 + p_b \cdot c_D \cdot x_5
 \end{aligned}$$

$$\begin{aligned}
 \dot{x}_5 &= p_f \cdot x_4 - [p_b \cdot c_D + l_f] x_5 + l_b \cdot x_6 \\
 \dot{x}_6 &= l_f \cdot x_5 - [l_b + g_{3f}] x_6 + g_{3b} \cdot c'_N \cdot x_7 \\
 \dot{x}_7 &= g_{3f} \cdot x_6 - [g_{3b} \cdot c'_N + g_{2f} + d_f + o_f \cdot c_s] \cdot x_7 \\
 & \quad + g_{2b} \cdot c'_N \cdot x_8 + d_b \cdot c_P \cdot x_{10} + o_b \cdot x_{11} \\
 \dot{x}_8 &= g_{2f} \cdot x_7 - [g_{2b} \cdot c'_N + g_{1f}] \cdot x_8 + g_{1b} \cdot c'_N \cdot x_9 \\
 \dot{x}_9 &= r_b \cdot c_P \cdot \frac{1}{P} \cdot x_1 + g_{1f} \cdot x_8 - [g_{1b} \cdot c'_N + r_f] \cdot x_9 \\
 \dot{x}_{10} &= e_b \cdot \frac{n_1 \cdot n_2}{P} \cdot x_1 + d_f \cdot x_7 - [d_b \cdot c_P + e_f] \cdot x_{10} \\
 \dot{x}_{11} &= o_f \cdot c_s \cdot x_7 - o_b \cdot x_{11}
 \end{aligned}$$

Because of the principle of microscopic reversibility, two rate constants were determined by the reaction cycles (e.g.,  $p_b$  and  $r_b$ , which are both difficult to obtain from experiments) (Langer, 1991; Wuddel, 1994).

Inasmuch as the kinetics of ATP release from caged ATP was in the time domain of the transport processes of interest, it had to be taken into account according to published findings (McCray et al, 1980; Borlinghaus and Apell, 1988)

$$\begin{aligned}
 c_T(t) &\equiv [\text{ATP}] = \vartheta \cdot [\text{cgATP}] \cdot (1 - e^{-\lambda t}) \cdot e^{-t/\tau_a} \\
 \lambda &= 2.2 \cdot 10^9 \cdot 10^{-\text{pH}} \cdot s^{-1}
 \end{aligned}$$

$\vartheta$  is the yield of ATP release from caged ATP, and  $\tau_a = 3$  s is an empirical determined constant, which depends on diffusion of ATP out of the vicinity of the membrane and on ATP hydrolysis by apyrase and the Na,K-ATPase.

The voltage dependence of the forward ( $k_f$ ) and backward ( $k_b$ ) rate constants is defined by

$$\begin{aligned}
 k_f(u) &= k_f(u=0) \cdot e^{\alpha u/2} \\
 k_b(u) &= k_b(u=0) \cdot e^{-\alpha u/2}
 \end{aligned}$$

$u = e_0 V/kT$  is the transmembrane voltage, expressed in units of  $kT/e_0 \cong 25$  mV, where  $k$  is the Boltzmann constant,  $T$  the absolute temperature,  $e_0$  the elementary charge, and  $\alpha$  the corresponding dielectric coefficient. In case of fast processes ( $\Delta t < 100$  ms), the membrane voltage could be assumed to be constant ( $V = V_{(t=0)}$ ). In longer lasting measurements, the time dependence of the voltage across the membrane fragments had to be taken into account

$$V = V_{(t=0)} \cdot e^{-t/\tau_v} \cdot v_s(t)$$

$\tau_v \cong 4.5$  s is the experimentally determined decay time of the voltage across the membrane fragments (see the Materials and Methods section), and  $v_s(t)$  is a normalized voltage across the compound membrane system and models mainly discharging processes of the bilayer membrane ( $v_s(0) = 1$ ).

To determine the initial conditions of the system differential equations, the solution of the linear equations  $\dot{x}_i = 0$  ( $i = 1, \dots, 11$ ) was solved with the substrate and voltage conditions before the experiment. A unique solution was found with the boundary condition  $\sum x_i = 1$ .

A modified Runge-Kutta algorithm was used to calculate the time-dependent solution of the states  $x_i$ . The pump current,  $I_p(t)$ , was determined as the sum of the fluxes of all electrogenic transitions

$$\begin{aligned}
 I_p(t) &= e_0 \cdot N \cdot \sum_i (\alpha_i \cdot \phi_i) \\
 \phi_i &= x_i \cdot k_f^i - x_{i+1} \cdot k_b^{i+1}
 \end{aligned}$$

$\alpha_i$  is the dielectric coefficient of transition  $i$ , and  $N$  is the number of active pump molecules in the adsorbed membrane fragments. In detail the electrogenic fluxes and in parentheses the corresponding dielectric constants were defined as:

$$\phi_{n3} = n_{3f}c_P \frac{n_1 n_2}{P} x_2 - n_{3b} x_3 \quad (\alpha)$$

$$\phi_1 = l_f x_5 - l_b x_6 \quad (\beta_0)$$

$$\phi_{g3} = g_{3f} x_6 - g_{3b} c_N'' x_7 \quad (\delta_0)$$

$$\phi_{g2} = g_{2f} x_7 - g_{2b} c_N'' x_8 \quad (\delta_1)$$

$$\phi_{g1} = g_{1f} x_8 - g_{1b} c_N'' x_9 \quad (\delta_2)$$

$$\phi_r = r_f x_9 - r_b c_P x_1 \quad (\gamma)$$

## REFERENCES

- Apell, H.-J. 1989. Electrogenic properties of the Na, K pump. *J. Membr. Biol.* 110:103–114.
- Bamberg, E., H.-J. Apell, N. Dencher, W. Sperling, H. Stieve, and P. Läuger. 1979. Photo currents generated by bacteriorhodopsin in planar lipid bilayer membranes. *Biophys. Struct. Mech.* 5:277–292.
- Barth, C., H. Bihler, M. Wilhelm, and G. Stark. 1994. Application of a fast charge-pulse technique to study the effect of the dipolar substance 2,4-D on the kinetics of valinomycin mediated  $K^+$ -transport across monoolein membranes. *Biophys. Chem.* 54:127–136.
- Benz, R., and K. Janko. 1976. Voltage-induced capacitance relaxation of lipid bilayer membranes. Effect of membrane composition. *Biochim. Biophys. Acta.* 455:721–738.
- Benz, R., and P. Läuger. 1976. Kinetic analysis of carrier-mediated ion transport by charge-pulse technique. *J. Membr. Biol.* 27:171–191.
- Borlinghaus, R., and H.-J. Apell. 1988. Current transients generated by the  $Na^+/K^+$ -ATPase after an ATP concentration jump: dependence on sodium and ATP concentration. *Biochim. Biophys. Acta.* 939:197–206.
- Borlinghaus, R., H.-J. Apell, and P. Läuger. 1987. Fast charge translocations associated with partial reactions of the Na,K-pump. I. Current and voltage transients after photochemical release of ATP. *J. Membr. Biol.* 97:161–178.
- Bühler, R., W. Stürmer, H.-J. Apell, and P. Läuger. 1991. Charge translocation by the Na, K-pump. I. Kinetics of local field changes studied by time-resolved fluorescence measurements. *J. Membr. Biol.* 121:141–161.
- Drachev, L. A., A. A. Jasaitis, A. D. Kaulen, A. D. Kondrashin, N. A. Liberman, I. B. Nemecek, S. A. Ostroumov, A. Y. Semenov, and V. P. Skulachev. 1974. Direct measurement of electric current generation by cytochrome oxidase,  $H^+$ -ATPase and bacteriorhodopsin. *Nature.* 249:321–324.
- Fendler, K., E. Grell, M. Haubs, and E. Bamberg. 1985. Pump currents generated by the purified  $Na^+, K^+$ -ATPase from kidney on black lipid membranes. *EMBO J.* 4:3079–3085.
- Forbush III, B. 1984.  $Na^+$  movement in a single turnover of the Na pump. *Proc. Natl. Acad. Sci. USA.* 81:5310–5314.
- Gadsby, D. C., R. F. Rakowski, and P. De Weer. 1993. Extracellular access to the Na, K pump: pathway similar to ion channel. *Science.* 260:100–103.
- Glynn, I. M. 1985. The  $Na^+, K^+$ -transporting adenosine triphosphatase. In *The Enzymes of Biological Membranes*, 2nd ed, Vol. 3. A. N. Martonosi, editor. Plenum, New York. pp. 35–114.
- Goldshleger, R., S. J. D. Karlish, A. Rephaeli, and W. D. Stein. 1987. The effect of membrane potential on the mammalian sodium-potassium pump reconstituted into phospholipid vesicles. *J. Physiol. (Lond.).* 387:331–355.
- Heyse, S., I. Wuddel, H.-J. Apell, and W. Stürmer. 1994. Partial reactions of the Na,K-ATPase: determination of rate constants. *J. Gen. Physiol.* 104:197–240.
- Hilgemann, D. W. 1994. Channel-like function of the Na, K pump probed at microsecond resolution in giant membrane patches. *Science.* 263:1429–1432.
- Jørgensen, P. L. 1974. Isolation of the  $(Na^+ + K^+)$ -ATPase. *Methods Enzymol.* 32:277–290.
- Jørgensen, P. L., and J. P. Andersen. 1988. Structural basis for  $E_1$ - $E_2$  conformational transitions in Na, K-pump and Ca-pump proteins. *J. Membr. Biol.* 103:95–120.
- Kaplan, J. H., B. Forbush III, and J. F. Hoffman. 1978. Rapid photolytic release of adenosine 5'-triphosphate from a protected analogue: utilization by the Na:K pump of human red blood cell ghosts. *Biochemistry.* 17:1929–1935.
- Läuger, P. 1991. *Electrogenic Ion Pumps*. Sinauer Associates, Sunderland, MA. 313 pp.
- Läuger, P., and H.-J. Apell. 1988. Voltage dependence of partial reactions of the  $Na^+/K^+$  pump: predictions from a microscopic model. *Biochim. Biophys. Acta.* 945:1–10.
- Lowry, O. H., N. J. Rosebrough, A. L. Farr, and R. J. Randall. 1951. Protein measurement with the Folin phenol reagents. *J. Biol. Chem.* 193:265–275.
- McCray, J. A., L. Herbette, T. Kihara, and D. R. Trentham. 1980. A new approach to time-resolved studies of ATP-requiring biological systems: laserflash photolysis of caged ATP. *Proc. Natl. Acad. Sci. USA.* 77:7237–7241.
- Nakao, M., and D. C. Gadsby. 1986. Voltage dependence of  $Na^+$  translocation by the Na/K pump. *Nature.* 323:628–630.
- Nakao, M., and D. C. Gadsby. 1989.  $[Na^+]$  and  $[K^+]$  dependence of the Na/K pump current-voltage relationship in guinea pig ventricular myocytes. *J. Gen. Physiol.* 94:539–565.
- Rakowski, R. F., L. A. Vasilets, J. La Tona, and W. Schwarz. 1991. A negative slope in the current-voltage relationship of the  $Na^+/K^+$  pump in *Xenopus* oocytes produced by reduction of external  $[K^+]$ . *J. Membr. Biol.* 121:171–187.
- Sagar, A., and R. F. Rakowski. 1994. Access channel model for the voltage dependence of the forward-running  $Na^+/K^+$  pump. *J. Gen. Physiol.* 103:869–894.
- Schulz, S., and H.-J. Apell. 1995. Investigation of ion binding to the cytoplasmic binding sites of the Na,K-pump. *Eur. Biophys. J.* 23:413–421.
- Schwartz, A., K. Nagano, M. Nakao, G. E. Lindenmayer, and J. C. Allen. 1971. The sodium- and potassium-activated adenosine triphosphatase system. *Methods Pharmacol.* 1:361–388.
- Stürmer, W., and H.-J. Apell. 1992. Fluorescence study on cardiac glycoside binding to the Na,K-pump: ouabain binding is associated with movement of electrical charge. *FEBS Lett.* 300:1–4.
- Stürmer, W., R. Bühler, H.-J. Apell, and P. Läuger. 1991. Charge translocation by the Na, K-pump: ion binding and release studied by time-resolved fluorescence measurements. In *The Sodium Pump. Recent Developments*. J. H. Kaplan and P. De Weer, editors. Rockefeller University Press, New York. 531–536.
- Vasilets, L. A., H. S. Omay, T. Otha, S. Noguchi, M. Kawamura, and W. Schwarz. 1991. Stimulation of the  $Na^+/K^+$  Pump by external  $[K^+]$  is regulated by voltage-dependent gating. *J. Biol. Chem.* 266:16285–16288.
- Wuddel, I. 1994. Untersuchung kinetischer und dielektrischer Eigenschaften der Na,K-ATPase: Hemmstoff und Ladungspuls-Experimente. Dissertation. University of Konstanz, Konstanz, Germany. 1–126.
- Wuddel, I., W. Stürmer, and H.-J. Apell. 1994. Dielectric coefficients of the extracellular release of sodium ions. In *The Sodium Pump. Structure Mechanism, Hormonal Control and Its Role in Disease*. E. Bamberg and W. Schoner, editors. Steinkopff, Darmstadt. 577–580.